FRET-Based Probe for Monitoring pH Changes in Lipid-Dense Region of Hct116 Cells

ARTICLE *in* ORGANIC LETTERS · NOVEMBER 2015

Impact Factor: 6.36 · DOI: 10.1021/acs.orglett.5b02568

6 AUTHORS, INCLUDING:

Upendar Reddy Gandra

CSIR - National Chemical Laboratory, Pune

10 PUBLICATIONS **160** CITATIONS

SEE PROFILE

Nandaraj Taye

National Centre For Cell Science, Pune

8 PUBLICATIONS **20** CITATIONS

SEE PROFILE

Amitava Das

CSIR - National Chemical Laboratory, Pune

195 PUBLICATIONS **4,702** CITATIONS

SEE PROFILE

Organic LETTERS

Letter

pubs.acs.org/OrgLett

FRET-Based Probe for Monitoring pH Changes in Lipid-Dense Region of Hct116 Cells

Upendar Reddy G,[†] Anila H. A,[†] Firoj Ali,[†] Nandaraj Taye,[‡] Samit Chattopadhyay,*[,‡] and Amitava Das*[,†]

[†]Organic Chemistry Division, CSIR-National Chemical Laboratory, Pune 411008, India

[‡]Chromatin and Disease Biology Laboratory, National Centre for Cell Science, Pune 411007, India

Supporting Information

ABSTRACT: A rhodamine conjugate (**L**) with a pseudo Stokes shift of 165 nm is used for probing changes in solution pH under physiological conditions. This reagent is found to be nontoxic, and the luminescence response could be used for imaging changes in endogenous pH induced by dexamethanose (DMT) in the endoplasmic reticulum.

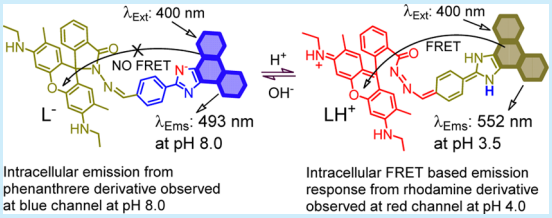

Very little is understood about the ionic composition of the endoplasmic reticulum (ER), one of the major compartments of the secretory pathway.[1] This has been primarily due to the inaccessibility of the ER to exogenous probes. It has been argued that the pH within individual organelles of the secretory pathway is an important factor for their biosynthetic activity. The importance of pH in the secretory pathway is also revealed by the adverse influence induced by inhibitors of the major organelles proton pump, the vacuolar H^+-ATPase.[2] The V-ATPase is an ATP-driven enzyme that transforms the energy of ATP hydrolysis to pump protons across diverse biological membranes via the primary active transport of H^+.[3]

There have been various attempts to measure the pH of the different compartments of the secretory pathway of different live cells. Because of the wide range of cells used and the different approaches adopted, little disparity has been noted in the reported pH of an individual compartment.[4] Despite such variations, absolute pH of the individual organelles has been defined with reasonable accuracy. The pH of the ER (pH^{ER}) is generally thought to be near neutral. However, the compartments of the secretory pathway become progressively more acidic thereafter, as the products of secretion approach their final destination.[5] Any deviation from such precisely maintained lumenal pH for the ER and the other compartments involved in the secretory pathway would experience disrupted activation of enzymes, sorting and processing of secretory proteins, lipid biosynthesis, and calcium storage.[6] These reports have clearly revealed that the pH within the individual organelles of the secretory pathway is crucial for their biosynthetic activity, and the precise measurement of the pH in the secretory organelles is essential. There are reports on new pH probes for monitoring minor pH changes in lysosome[7] and mitochondria.[8] To the best of our knowledge, examples of a molecular probe capable of noninvasive dynamic measurement of pH in the lumen of the ER, a lipid dense region, are scarce in contemporary literature.[9] The first report estimating the pH of the ER revealed that it was achieved by quantifying the partition of a permeant weak base by immunoelectron microscopy.[10] Other attempts to develop an efficient ER-specific fluorescent probe are mostly restricted to the utilization of probes for monitoring ER redox poise using derivatives of green fluorescent proteins with a small Stokes shift value.[11] Recently, a naphthalenediimide-based imaging reagent with Stokes shifts of ~75 nm was reported for estimation of the pH of the ER (pH^{ER}) in aq buffer−DMSO (9:1, v/v) medium.[9a] Parker and co-workers have reported an unique UV-excitable Eu(III)-based reagent for probing changes in intracellular pH with delayed longer wavelength emission.[9b] However, an example of a FRET (Förster resonance energy transfer)-based, ER-specific fluorescent probe has still eluded us, despite the obvious desirability of a FRET-based receptor over a simple fluorescence-based receptor.[12]

It has been argued by many researchers that the evaluation of the change in pH^{ER} also provides information on overall cytosolic pH. Thus, design of an ER-specific imaging reagent that shows a FRET-based response for monitoring changes in intracellular pH has significance. In this report, we discuss a new molecular probe (**L**, Scheme 1) for probing changes in pH^{ER} based on FRET mechanism. To the best of our knowledge, there is no such report available in contemporary literature. Details about the synthesis

Scheme 1. Partial Methodology That Was Adopted for Synthesis of L and Molecular Structures for A, B, R, and L

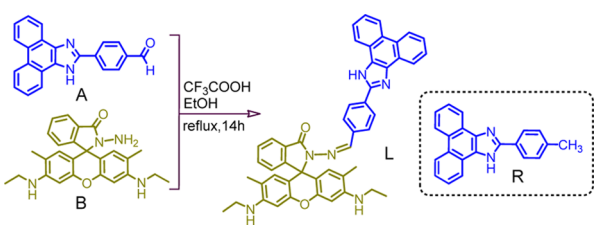

Received: September 5, 2015

DOI: 10.1021/acs.orglett.5b02568
Org. Lett. XXXX, XXX, XXX−XXX

and characterization of the reagent **L** are provided in the Supporting Information (SI).

The absorption and emission spectra of **L** (10 μM) were recorded in aq PBS buffer−DMSO (98:2, v/v, pH 7.0) solution. An intense absorption band was observed at 388 nm for $\pi-\pi^*$-based transition of the imidazole derivative of the phenanthrene moiety (Figure 1). An electronic spectral band with maxima at

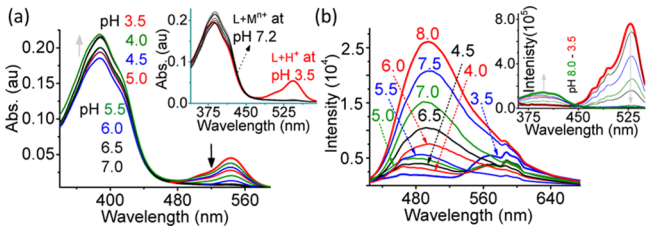

Figure 1. Systematic changes in (a) absorption and (b) emission spectra (λ_{Ext} = 400 nm; slit: 1/1 nm) for **L** (10 μM) at different pH (3.5−8.0). Inset (a): absorbance spectra of **L** (10 μM) in the absence and the presence of 30 molar equiv of different metal ions (M^{n+}= Na^+, K^+, Mg^{2+}, Hg^{2+}, Cu^{2+}, Zn^{2+}, Cr^{3+}, Fe^{3+}, Co^{2+}, Cr^{3+}, Pd^{2+}, Pb^{2+}, Ni^{2+}, Cd^{2+}), glutathione (GSH), cysteine (Cys), and homocysteine (Hcy) at pH 7.2 as well as at pH 3.5). Inset (b): excitation spectra of **L** (10 μM) for λ_{Ems} of 552 nm and this confirms its dual excitation ratiometric pH sensing ability. All studies were performed in aq PBS buffer−DMSO (98:2, v/v) medium.

~380 nm for the model reagent **R** confirmed this assignment. This further corroborated the fact that **L** was present exclusively in its spirolactam form at pH 7.0 and accounted for its colorless solution. A characteristic signal at ~65.89 ppm for the tertiary C atom in the ^{13}C NMR spectrum for **L** also confirmed its spiro lactam structure (SI).[13]

Figure 1a clearly reveals that a new absorption band with maximum at 542 nm appears at with gradual decrease in solution pH from 7.0 to 3.5. At pH 7.0, reagent **L** was present exclusively in the cyclic lactam form,[13] while the acyclic xanthene form of LH^+ prevailed at pH 3.5 (Figure 2) and this was attributed to the visually detectable change in the absorption spectra (Figure 1a). Such a change was not observed when spectra were recorded in presence any other analytes that were used for the present study (Figure 1a, inset).

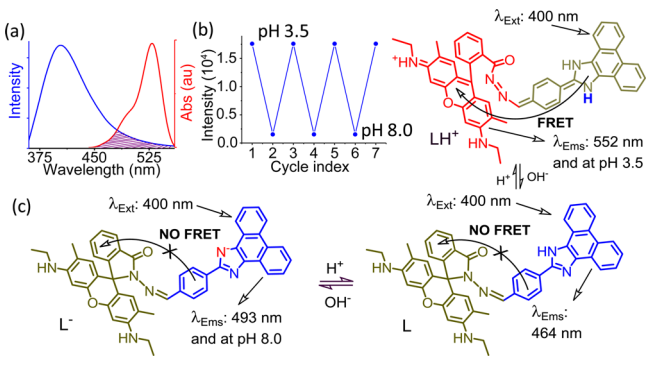

Figure 2. (a) Overlap spectra for an emission and an absorption spectrum of the donor (**R**) and acceptor acyclic form BH^+, respectively; (b) reversible fluorescence changes of **L** (10 μM) between pH 3.5 and pH 8.0 (λ_{Ext}: 505 nm) in aq PBS buffer−DMSO (98:2, v/v) medium at 25 °C; (c) schematic presentation of the different forms that **L** could exist at different media pH.

Luminescence spectra for **L** were also recorded in the presence of all of the above referred metal ions and thio amino acids at pH 7.0 in aq PBS buffer−DMSO (98:2, v/v) medium (SI), and no change in the emission spectral pattern was observed. However, the spectrum observed at pH 3.5 was typical for the acyclic form the rhodamine derivative.[13] Interference studies were performed by recording emission spectra of **L** at pH 3.5 in an essentially aq buffer medium in the presence of higher concentration of the above-referred metal ions, GSH, Cys, and Hcy (SI). Results of such studies clearly revealed that the luminescence response of the reagent **L** toward media pH remained unaltered due the presence of the probable interfering cations/thio amino acids. A luminescence band at ~493 nm (λ_{Ext}: 400 nm) was observed for **L** at media pH of 7.0, while the emission band for the model reagent **R** with lower extended conjugation appeared at 425 nm under identical experimental conditions. These helped us to conclude that the band maximum at 493 nm for **L** was associated with the transitions of the substituted imidazole derivative (Figures 1b and 2b). Further, excitation spectra of **L** (10 μM) (λ_{Ems} = 552 nm) confirmed the dual excitation ratiometric pH sensing ability of the reagent **L** (Figure Inset 1b).

As discussed previously, reagent **L** existed as a cyclic lactam derivative and did not show any detectable emission band following excitation at ~505 nm at pH 7.0. Figure 1b also reveals that on lowering the solution pH from 8.0 to 3.5 a gradual bleach in emission intensity at 493 nm (λ_{Ext}: 400 nm) is observed (Figure 1b) with concomitant increase of a new emission band around 550−610 nm on excitation at 400 nm. This growth in emission band around 550−610 nm is primarily due the formation of LH^+ (Figure 1b and 2c). Similar growth in emission intensity was also observed in emission spectra following excitation at 505 nm (SI), though the relative emission quantum yields (Φ) were found to be different ($\Phi[\lambda_{Ext}400\text{ nm}] = 0.02$ and $\Phi[\lambda_{Ext}505\text{ nm}] = 0.78$; rhodamine 6G was used as standard). Studies also revealed that there was a definite spectral overlap between the emission spectra of the model reagent **R** and the analogous rhodamine derivative (BH^+), an essential condition for the FRET process. A steady-state emission spectrum for a physical mixture containing equimolar amounts two model reagents (**R** and BH^+) was basically a summation of the spectra of two independent luminophores (SI), and this nullified any possibility for the intermolecular energy transfer process. Thus, the observed emission band with λ_{Max} at 552 nm for the aq buffer solution of **L** (λ_{Ext} of 400 nm) at pH ≤ 6.5 could only be explained by the FRET-based response. Efficiency of the FRET process between donor imidazole and the acceptor rhodamine moieties in **L** was evaluated to be 42% from the steady-state emission data (SI).[14] Conversion from cyclic (**L**) to the acyclic (LH^+) form (Figure 2c) was accounted for the first set of pH changes from 3.5 to 5.5 with an isoemission point at 540 nm, while deprotonation at the $HN_{Imidazole}$ moiety in **L** accounted for the observed increase in emission intensity at ~490 nm (Figures 1b and 2c). The observed difference of 165 nm between the donor absorption (388 nm) and the acceptor emission (553 nm) for LH^+ (pH ≤ 5.0; Figure 1b) could be referred as the pseudo Stokes shift (ΔSs), and this compares well with FRET-based receptors reported to date for any visible light excitable molecular probe.[7k,l] The choice of rhodamine 6G derivative over rhodamine B derivative helped us in achieving the spectral overlap and the FRET-based response in the present study.[13c] Recently, a new receptor was reported that shows a FRET-based response on specific change in solution as well as lysosomal pH (6.0 to 4.2) with a pseudo ΔSs of 105 nm.[7m] There are other

DOI: 10.1021/acs.orglett.5b02568
Org. Lett. XXXX, XXX, XXX−XXX

examples on lysosome-specific rhodamine-based pH probe.[7k−m] However, no ER-specific pH probe with FRET response has been reported to date.[15] Reversibility of the luminescence responses (λ_{Ext}: 505 nm; Figure 2b) was also established for the solution pH 3.5−8.0.

MTT assay studies confirmed insignificant toxicity of **L** toward live Hct116 cells (SI). After ensuring the FRET-based luminescence response of the biologically benign and visible light excitable reagent **L** toward media pH, the possibility of using this reagent for tracking intracellular pH of Hct116 cells was explored using confocal laser scanning microscopic (CLSM) studies (Figure 3). Analysis of CLSM images of Hct116 cells,

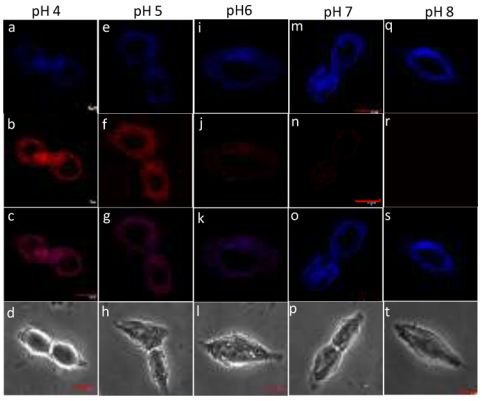

Figure 3. CLSM images recorded for Hct116 cells maintained at pH 4 (a−d), 5 (e−h), 6 (i−l), 7 (m−p), and 8 (q−t) using probe **L** (10 μM). The excitation wavelength was 400 nm, and the images were collected at 460 nm (blue channel; first row) and 586 nm (red channel; second row). Ratio images obtained from the blue and red channels (third row) and the corresponding bright field images (fourth row).

stained with the reagent **L**, revealed distinctly different intracellular emission responses from cells incubated at different media pH. For cells that were incubated in media having pH 4.0, only red intracellular emission, primarily from the acyclic form of the reagent $\mathbf{LH}^+$ (Figure 2c), was observed when images were viewed using red channel, and a weak intracellular emission was observed when viewed through blue channel (Figure 3). Analogous studies for media pH of 8.0 showed distinct blue intracellular emission (for $\mathbf{L}^-$) when viewed through the blue channel, and no intracellular emission was observed when red channel was used (Figure 3). These observations agreed well with the emission responses of the reagent **L** toward solution pH (Figure 1). Figure 3 further revealed that on gradual increase in media pH from 4.0 to 8.0, in which Hct116 cells were incubated, a gradual increase in blue intracellular emission was observed (using blue channel) with a concomitant decrease in red intracellular emission (using red channel). Intracellular emissions were observed at both channels for Hct116 cells incubated at pH 6.0 (Figure 3i,j). Thus, above-described results clearly revealed that the reagent **L** could be used as FRET-based dual imaging probe for monitoring the changes in intracellular pH (4.0−8.0). Further, colocalization experiments were performed using **L** and organelle-specific fluorescent dye (ER Tracker Green; ERTG) to identify the location or localization of the reagent **L** in Hct116 cells, which accounted for the intracellular blue and red fluorescence. Close comparison of these images as well as the images of the costaining experiments with ERTG (Figure 4a−d) clearly revealed that intracellular emissions for **L** were found to be exactly superimposed with those for ERTG and distributed mainly in the lipid dense region of ER.

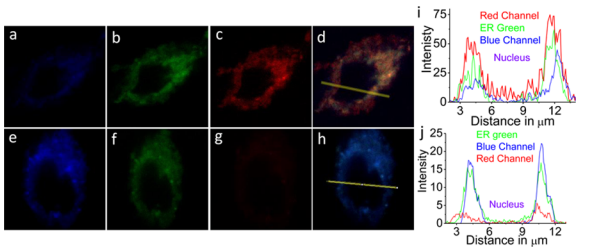

Figure 4. Co-localization experiments using reagent **L** and ER-Tracker green (ERTG) in Hct116 cells. Cells were incubated with **L** (10 μM) for 20 min at 37 °C, and the medium was replaced with fresh medium containing ERTG (1 μM) and incubated for 30 min. CLSM images with reagent **L** were collected for the blue channel and red channel following excitation with a laser source of 400 nm. CLSM images with ERTG (b and f) were recorded using a laser excitation source of 495 nm and emission filter of 519 nm; d and h are the merged images of (a,b and c) and (e,f and g), respectively. First row images were collected at pH 5.0, and second row images were collected at pH 7.2 medium; (i) and (j) are line profiles cell Hct116 cell revealing specific staining in the lipid dense ER-region around nucleus.

Interestingly, for intracellular pH ≥ 7.0, no FRET-based red emission from $\mathbf{L}^-$ was observed. Hct116 cells incubated with solution having pH ≤ 6.0 revealed a strong FRET-based red emission, while emission intensity was enhanced with lowering of the media pH. Further, Pearson's correction coefficient (Pcc) was evaluated from the overlay of CLSM images of Hct116 cells stained with **L** and ERTG. These evaluated Pcc were 0.94 (586 nm filter) and 0.76 (460 nm filter) at pH 5.0 and 0.96 (586 nm) and 0.12 (460 nm filter) at pH 7.2. This confirmed that the reagent **L** was solely localized in the ER region of the Hct116 cells. This also confirmed that the FRET based intracellular luminescence response was operational at pH 5.0. Presumably, the higher lipophilicity has favored the specific localization of the reagent (**L**) in the lipid dense region (ER) of the Hct116 cells (SI). To the best of our knowledge, this is the first report on an imaging reagent that is capable of monitoring changes in pH in ER of Hct116 cells. FRET-based response has further enhanced its significance.[9]

Intracellular acidification is closely associated with cell growth and apoptosis.[15] DMT is known to lower the pH of the cytosol by inhibiting the H^+-ATPase activity and by probing the change in pH in the ER region one could gain insight about the overall change in cytosolic pH.[9b,16] H^+-ATPase accounts for maintaining the optimum cellular pH. It has been argued that DMT interferes with the H^+-ATPase activity and reduces the intracellular pH, which eventually causes cell apoptosis. We performed some preliminary studies to check the feasibility of monitoring changes in intracellular pH induced by DMT. Live Hct116 cells were pre-exposed to an aq PBS buffer solution (pH 7.2) of **L** (10 μM) for 20 min, in the absence and presence of DMT (2 μM). These cells were then subjected to CLSM studies, and more intense red intracellular luminescence was observed for cells loaded with DMT (Figures 5a-5f).

Linearity of the luminescence responses at 490 or 552 nm (λ_{Ext}: 400 nm) was confirmed for pH range 3.5−8.0, and for this particular set of experiments, fixed Hct116 cells treated with Titron-X100 were used. A plot of ratio of intensity of the confocal image (when viewed through red and blue channels) at respective pH vs pH (SI for methodology) helped us in

DOI: 10.1021/acs.orglett.5b02568
Org. Lett. XXXX, XXX, XXX−XXX

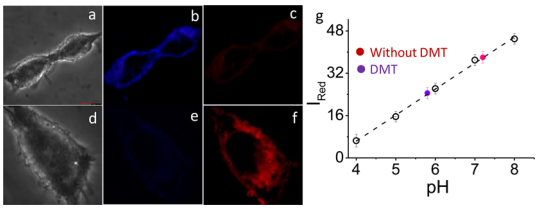

Figure 5. CLSM images of live Hct116 cells incubated with **L** (10 μM): (a–c) control experiment without using DMT, (a) bright field image, (b and c) images observed in the blue and red channels; (d–f) experiments with live Hct116 cells in the presence of DMT (2 μM); (d) bright field image, (e and f) images observed in the blue and red channel. (g) Intracellular pH calibration curve of probe **L** in fixed Hct116 cells obtained from red fluorescence intensity (I_{red}) of cells exposed to different media pH, and each data point is an average of three independent measurements.

generating a calibration plot (Figure 5g). This calibration curve was used for measuring possible intracellular pH, which was evaluated as 7.2 ± 0.2 and 5.9 ± 0.2, respectively, before and after treatment with 2 μM DMT for 20 min. This value seems to be in line with a previous report, which suggests that use of 1 nM DMT could lower the intracellular pH to 6.4 for 16HBE14o$^-$ cells on incubation for 12 min.[15b] Thus, result of this preliminary study clearly revealed that DMT was responsible for lowering of the cellular pH and the reagent **L** could be used for monitoring this change in intracellular pH.

Briefly, we have reported a unique FRET-based ER specific imaging probe with a pseudo-Stokes shift of 165 nm for monitoring pH changes in aqueous buffer medium under physiological conditions and for measuring the endogenous pH of the lipid dense region of the Hct116 cells. This reagent could be used for probing the change in intracellular pH in the ER region of the Hct116 cells induced by DMT.

■ ASSOCIATED CONTENT

Supporting Information

The Supporting Information is available free of charge on the ACS Publications website at DOI: 10.1021/acs.orglett.5b02568.

Experimental details, synthesis, and characterization of ^{1}H NMR, ^{13}C NMR, and mass analysis (PDF)

■ AUTHOR INFORMATION

Corresponding Authors

*E-mail: samit@nccs.res.in.
*E-mail: a.das@ncl.res.in.

Notes

The authors declare no competing financial interest.

■ ACKNOWLEDGMENTS

A.D. acknowledges a SERB (India) grant (SB/S1/IC-23/2013) and CSIR-NCL for funds through Project MLP-028226. U.R.G. and A.H.A. acknowledge UGC, while N.T. acknowledges CSIR for their research fellowships.

■ REFERENCES

(1) Kim, J. H.; Johannes, L.; Goud, B.; Antony, C.; Lingwood, C. A.; Daneman, R.; Grinstein, S. *Proc. Natl. Acad. Sci. U. S. A.* **1998**, *95*, 2997.

(2) (a) Yilla, M.; Tan, A.; Ito, K.; Miwa, K.; Ploegh, H. L. *J. Biol. Chem.* **1993**, *268*, 19092. (b) Serrano, A.; Pérez-Castiñeira, J. R.; Baltscheffsky, M.; Baltscheffsky, H. *IUBMB Life* **2007**, *59*, 76.

(3) Beyenbach, K. W.; Wieczorek, H. *J. Exp. Biol.* **2006**, *209*, 577.

(4) Paroutis, P.; Touret, N.; Grinstein, S. *Physiology* **2004**, *19*, 207.

(5) Wu, M. M.; Grabe, M.; Adams, S.; Tsien, R. Y.; Moore, H. P.; Mache, T. E. *J. Biol. Chem.* **2001**, *276*, 33027.

(6) (a) Mellman, I.; Fuchs, R.; Helenius, A. *Annu. Rev. Biochem.* **1986**, *55*, 663. (b) Halban, P. A.; Irminger, J. C. *Biochem. J.* **1994**, *299*, 1. (c) Schmidt, W. K.; Moore, H. P. *Mol. Biol. Cell* **1995**, *6*, 1271. (d) Brown, M. K.; Naidoo, N. *Front. Physiol.* **2012**, *3*, 1.

(7) (a) Lee, M. H.; Han, J. H.; Lee, J. H.; Park, N.; Kumar, R.; Kang, C.; Kim, J. S. *Angew. Chem., Int. Ed.* **2013**, *52*, 6206. (b) Wan, Q.; Chen, S.; Shi, W.; Li, L.; Ma, H. *Angew. Chem., Int. Ed.* **2014**, *53*, 10916. (c) Wu, S.; Li, Z.; Han, J.; Han, S. *Chem. Commun.* **2011**, *47*, 11276. (d) Zhu, H.; Fan, J.; Xu, Q.; Li, H.; Wang, J.; Gao, P.; Peng, X. *Chem. Commun.* **2012**, *48*, 11766. (e) Fan, J.; Dong, H.; Hu, M.; Wang, J.; Zhang, H.; Zhu, H.; Sun, W.; Peng, X. *Chem. Commun.* **2014**, *50*, 882. (f) Ho, Y. M.; Au, N. P.; Wong, K. L.; Chan, C. T.; Kwok, W. M.; Law, G. L.; Tang, K. K.; Wong, W. Y.; Ma, C. H.; Lam, M. H. *Chem. Commun.* **2014**, *50*, 4161. (g) Wang, L.; Xiao, Y.; Tian, W.; Deng, L. *J. Am. Chem. Soc.* **2013**, *135*, 2903. (h) Li, Z.; Song, Y.; Yang, Y.; Yang, L.; Huang, X.; Han, J.; Han, S. *Chem. Sci.* **2012**, *3*, 2941. (i) Nakagawa, A.; Hisamatsu, Y.; Moromizato, S.; Kohno, M.; Aoki, S. *Inorg. Chem.* **2014**, *53*, 409. (j) Kim, H. J.; Heo, C. H.; Kim, H. M. *J. Am. Chem. Soc.* **2013**, *135*, 17969. (k) Shen, S. L.; Chen, X. P.; Zhang, X. F.; Miao, J. Y.; Zhao, B. X. *J. Mater. Chem. B* **2015**, *3*, 919. (l) Zhang, X. F.; Zhang, T.; Shen, S. L.; Miao, J. Y.; Zhao, B. X. *J. Mater. Chem. B* **2015**, *3*, 3260. (m) Zhang, X. F.; Zhang, T.; Shen, S. L.; Miao, J. Y.; Zhao, B. X. *RSC Adv.* **2015**, *5*, 49115. (n) Zhang, J.; Yang, M.; Li, C.; Dorh, N.; Xie, F.; Luo, F. T.; Tiwari, A.; Liu, H. *J. Mater. Chem. B* **2015**, *3*, 2173.

(8) (a) Lee, M. H.; Park, N.; Yi, C.; Han, J. H.; Hong, J. H.; Kim, K. P.; Kang, D. H.; Sessler, J. L.; Kang, C.; Kim, J. S. *J. Am. Chem. Soc.* **2014**, *136*, 14136. (b) Chattoraj, S.; Chowdhury, R.; Dey, S. K.; Jana, S. S.; Bhattacharyya, K. *J. Phys. Chem. B* **2015**, *119*, 8842. (c) Zhang, Q.; Cao, R.; Fei, H.; Zhou, M. *Dalton Trans.* **2014**, *43*, 16872. (d) Chen, Y.; Zhu, C.; Cen, J.; Bai, Y.; He, W.; Guo, Z. *Chem. Sci.* **2015**, *6*, 3187.

(9) (a) Ghule, N. V.; Bhosale, R. S.; Kharat, K.; Puyad, A. L.; Bhosale, S. V.; Bhosale, S. V. *ChemPlusChem* **2015**, *80*, 485. (b) McMahon, B. K.; Pal, R.; Parker, D. *Chem. Commun.* **2013**, *49*, 5363. (c) Meinig, J. M.; Fu, L.; Peterson, B. R. *Angew. Chem., Int. Ed.* **2015**, *54*, 9696.

(10) Orci, L.; Ravazzola, M.; Amherdt, M.; Madsen, O.; Perrelet, A.; Vassalli, J.-D.; Anderson, R. G. *J. Cell Biol.* **1986**, *103*, 2273.

(11) Birk, J.; Ramming, T.; Odermatt, A.; Herzog, C. A. *Front. Genet.* **2013**, *4*, 1. Vilozny, B.; Schiller, A.; Wessling, R. A.; Singaram, B. *J. Mater. Chem.* **2011**, *21*, 7589.

(12) (a) Fan, J.; Hu, M.; Zhan, P.; Peng, X. *Chem. Soc. Rev.* **2013**, *42*, 29. (b) Yuan, L.; Lin, W.; Zheng, K.; Zhu, S. *Acc. Chem. Res.* **2013**, *46*, 1462. (c) Wu, Y.-X.; Zhang, X.-B.; Li, J.-B.; Zhang, C.-C.; Liang, H.; Mao, G. J.; Zhou, L.-Y.; Tan, W.; Yu, R. Q. *Anal. Chem.* **2014**, *86*, 10389. (d) Meier, R. J.; Simburger, J. M. B.; Soukka, T.; Schaferling, M. *Chem. Commun.* **2015**, *51*, 6145.

(13) (a) Mahato, P.; Saha, S.; Das, P.; Agarwalla, H.; Das, A. *RSC Adv.* **2014**, *4*, 36140. (b) Saha, S.; Mahato, P.; Reddy, G. U.; Suresh, E.; Chakrabarty, A.; Baidya, M.; Ghosh, S. K.; Das, A. *Inorg. Chem.* **2012**, *51*, 336. (c) Reddy G, U.; Ramu, V.; Roy, S.; Taye, N.; Chattopadhyay, S.; Das, A. *Chem. Commun.* **2014**, *50*, 14421. (d) Praveen, L.; Saha, S.; Jewrajka, S. K.; Das, A. *J. Mater. Chem. B* **2013**, *1*, 1150. (e) Mahato, P.; Saha, S.; Das, P.; Agarwal, H.; Das, A. *RSC Adv.* **2014**, *4*, 36140. (f) Ali, F.; Saha, S.; Maity, A.; Taye, N.; Si, M. K.; Suresh, E.; Ganguly, B.; Chattopadhyay, S.; Das, A. *J. Phys. Chem. B* **2015**, *119*, 13018.

(14) Reddy G, U.; Lo, R.; Roy, S.; Banerjee, T.; Ganguly, B.; Das, A. *Chem. Commun.* **2013**, *49*, 9818.

(15) Zhou, X.; Su, F.; Lu, H.; Willis, P. S.; Tian, Y.; Johnson, R. H.; Meldrum, D. R. *Biomaterials* **2012**, *33*, 171. (b) Verrière, V. A.; Hynes, D.; Faherty, S.; Devaney, J.; Bousquet, J.; Harvey, B. J.; Urbach, V. *J. Biol. Chem.* **2005**, *280*, 35807.

(16) (a) Nauclér, C.; Sundler, R.; Tapper, H. *J. Leukocyt. Biol.* **2000**, *67*, 876. (b) Gill, M. R.; Cecchin, D.; Walker, M. G.; Mulla, R. S.; Battaglia, G.; Smythe, C.; Thomas, J. A. *Chem. Sci.* **2013**, *4*, 4512.

DOI: 10.1021/acs.orglett.5b02568
Org. Lett. XXXX, XXX, XXX–XXX